

A Focal Mechanism Diagram Generator for Analysis of Earthquake First Motions

Declan G. De Paor

Department of Physics, Worcester Polytechnic Institute, Worcester MA 01609

Email: declan@wpi.edu

Elizabeth Wilson

Department of Earth Sciences, Boston University, Boston MA 02215

Heather Melanson

Department of Earth Sciences, Boston University, Boston MA 02215

Keywords: XML, geophysics, earthquakes, focal mechanism, first motion, moment tensor solution, geophysical beach ball, visualization, Flash™, ActionScript™

Abstract: We present an interactive method for analyzing earthquake first motions and generating focal mechanism diagrams using Flash Actionscript™. A shockwave flash movie file call FirstMo.swf monitors first arrival data stored in an external data file. Data may be in the form of XML-tagged arrival directions (plunge, trend, and up/down ground motion), or the data may be plotted on a stereographic projection and imported as a jpeg image. Variables under user control include nodal plane orientations, moment magnitude scale, transparency, and background map. Focal depths are color-coded using a standard UGSG look-up table.

Tsunamigenic earthquakes have characteristic moment tensor solutions, thus rapid rendering and enhanced visualization of focal mechanism diagrams may help with the dissemination of critical information to public safety personnel and the general public.

Table of Contents

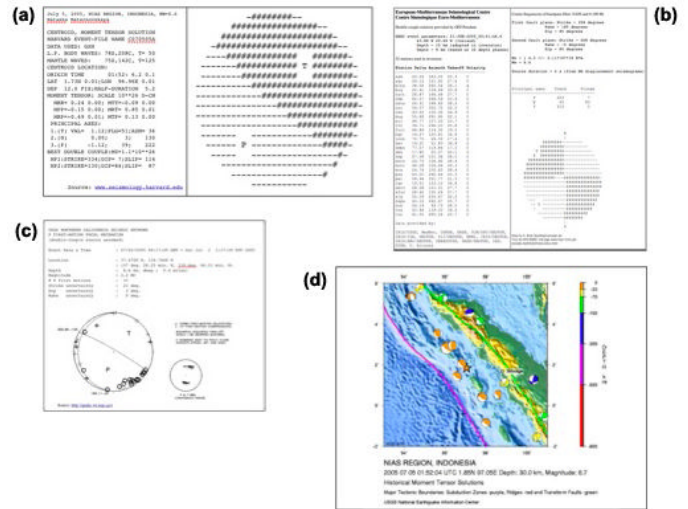
Introduction	4
Background	5
Data Format	6
Fitting the Focal Mechanism to the data	8
Exporting Data	8
Conclusions	9
References	9

Introduction

As illustrated by Figure 1, many earthquake monitoring web sites present focal mechanism data using line-printer style output reminiscent of the earliest computer graphics. Some sites – notably the USGS and General Mapping Tools – employ sophisticated graphical interfaces and advanced visualization tools, but results are usually presented as static jpeg files that are not editable or linked to the source data. A survey of web sites in Table 1 demonstrates that the presentation of focal mechanism solutions is widespread but not generally graphically sophisticated. Determination of focal mechanisms for major earthquakes and their aftershocks is critical to our understanding of neotectonics (e.g., McNutt & Sánchez, 2000, Lisa, et al. 2004). Indeed, this may be a matter of life and death, as tsunami-genic earthquakes exhibit characteristic focal mechanisms as well as magnitudes. Rapid publication of moment tensor solutions in a graphical format that is easily understood by public safety officials and citizens is thus a priority. We therefore undertook a programming project to facilitate the construction of focal mechanism solutions (so-called geophysical beach balls) through an interactive web-based flash movie, and to overlay multiple moment tensor solutions on maps using real-time monitoring of data stored in XML files on the Internet.

In the first of a planned series of papers, we here present a focal mechanism generator for use with raw first arrival data. Subsequent papers will enable rendering of multiple (tens or hundreds) of moment tensor solutions on a background map, and will address the incorporation of moment tensor solutions into klm / kmz files viewable with Google Earth™ software. This undergraduate research opportunity was funded by a grant from the National Science Foundation, EAR 0310232: "Real-time Monitoring, Enhanced Visualization and Temporal Analysis of Tectonic and Geophysical Data."

Figure 1. Screens



a) Focal mechanism output from Harvard Seismological Group <http://www.seismology.harvard.edu>

b) Data from USGS Earthquake Hazards Program <http://www.quake.wr.usgs.gov>

c) Focal mechanism output from GEOFON program at Potsdam <http://www.gfz-potsdam.de/geofon>

d) Jpeg map with beach balls from USGS (<http://neic.usgs.gov>)

Sample web sites featuring focal mechanism solutions

- http://www.sg.geophys.ethz.ch/geodynamics/klaus/WS_20_00/Lithosphere/Dynamics%20III_files/image014.jpg
- <http://www.orfeus-eu.org/newsletter/vol6no1/bam.html>
- <http://pubs.usgs.gov/of/2002/ofr-02-0073/images/Slides22.gif>
- http://www.hinet.bosai.go.jp/topics/niigata041023/mechanisms_j.html
- <http://cais.gsi.go.jp/YOCHIREN/JIS/141/Gif/141-11.gif>
- http://www-geology.ucdavis.edu/~gps/GMT/LONG_VALLEY/LV_focal_mech.JPG
- http://www.hdip.com.pk/MonaLisa-PJHR_files/image010.gif
- <http://pubs.usgs.gov/pinatubo/bbautist/fig9.gif>
- http://www.earth.sinica.edu.tw/~smdmc/recent/2002/special_eqk.jpg

- <http://www-seis.planet.sci.kobe-u.ac.jp/~harada/hypoDD.epi.jpg>
- http://www-geology.ucdavis.edu/~gps/GMT/gmt_intro.html
- http://www-geology.ucdavis.edu/~gps/GMT/LONG_VALLEY/hypocenter.html

Background

Earthquakes frequently involve a simple double-couple motion (e.g., Sherburne & Cramer, 1984, Cronin 2004; see also, <http://earthquake.usgs.gov/learning/glossary.php>), meaning that slip movement is confined to a direction parallel to a planar failure surface (either an existing fault plane or a newly formed fracture), with no component of motion perpendicular to the plane. The combination of a specific failure plane and a slip direction for the oscillatory motion along that plane is called a focal mechanism, and is analogous to a slip system in crystal lattice-scaled deformation mechanism studies.

Fault slip initiates at a point, the focus or hypocenter. The disturbance propagate radially, both through the surrounding body of the rock and along the surface, as a complex set of elastic waves that are recorded at receiver stations around the globe. The wave packages that penetrate the earth include push-pull, or P-waves, traveling at velocity

$$V_p = \sqrt{k + 1.33m/r}$$

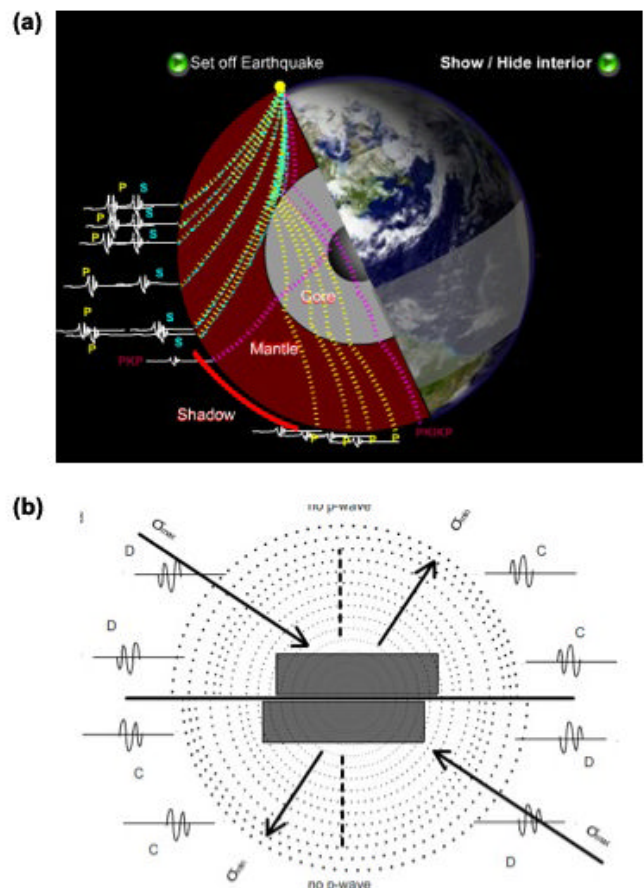
and sideways-shearing, or S-waves, traveling at velocity

$$V_s = \sqrt{m/r}$$

where k is the bulk modulus (resistance to pressure waves), m is the shear modulus (resistance to shear waves), and r is the rock density. Typical values for granite and peridotite are $k = 88 - 139 \times 10^9 \text{ N/m}^2$, $m = 22 - 58 \times 10^9 \text{ N/m}^2$, and $r = 2.6 - 3.3 \text{ gm/cc}$, yielding crustal and mantle velocities of $V_p = 6.7 - 8.1 \text{ km/s}$ and $V_s = 2.9 - 4.2 \text{ km/s}$ (e.g., Lillie, 1999). Thus the first arrivals at seismic stations, some minutes to tens of minutes after the seismic

event, are the faster P-waves and the initial deflection they create on seismographs are called first motions (Fig. 2a). A first motion emerging from the earth at a seismic station may either shorten crystal bonds in the displacement direction, leading to compressional stress (and a "down" tick of the seismograph), or it may lengthen bonds, leading to tensile stress (and an "up" tick on the seismograph). With classical paper roll seismographs, inertia causes the pen to remain fixed while the rest of the instrument shifts, resulting in an down tick of the ink line when the ground motion is up and vice versa. Modern computerized equipment flips the record, so that an up tick of the graph denotes upward ground motion.

Figure 2. Quake screens



a) After an event, first arrivals at seismic stations around the globe are always P-waves. S-waves lag behind as a function of distance and are blocked completely by the outer core. Click here (FIXME) to run the shockwave flash animation. photo source: NASA.

b) First motions recorded from dextral slip on a fault plane (bold horizontal line). C's denote compressional

and D's denote dilatational first arrivals. Seismographs are drawn from left to right. There are no p-wave arrivals in the direction of the auxiliary plane (dashed line). Arrows indicate principal stresses s_{max} and s_{min} (which is shown as a tension in this case). Dotted circles are initially concentric passive markers. Click here (FIXME) to run the shockwave flash animation.

If seismic stations were distributed uniformly about a hypothetical sphere called the focal sphere, centered on the hypocenter, we would expect compressional first motion arrivals (labeled C) and dilatational first motion arrivals (labeled D) to be distributed in quadrants as in Fig. 2b (ignoring deflections due to detailed mantle or crustal structure). The compressed quadrants are conventionally shaded black, and the dilated quadrants are left white, creating the appearance of a beach ball (e.g., USGS 1996). The beach ball quadrants are bounded by two great circles representing the nodal planes. One of these is the fault plane and the other is called the auxiliary plane. Assuming, for simplicity, that failure occurs on planes of maximum shear stress, the maximum (compressive) and minimum (tensile) principal axes of the stress ellipsoid bisect the dihedral angles subtended by the nodal planes, while the intermediate principal stress is aligned along their intersection. Note that the maximum principal stress (compression) lies in the dilated quadrants whereas the minimum principal stress (which may be a smaller compressive or a tensile stress) lies in the compressed quadrants.

The above stress orientation is equally valid for slip on either nodal plane. We are thus faced with an ambiguity when we try to determine the focal mechanism given scattered first motion data. Small quakes, aftershocks, and general tectonic setting may help distinguish the fault plane from the auxiliary plane. For example, faults in thrust belts commonly dip at 30° or less whereas normal faults dip $60\text{--}70^\circ$. According to the Mohr-Coulomb failure criterion, the maximum stress axis is actually oriented at less than 45° to the fault plane, and the amplitudes of ground motions are greater for receiver stations oriented near the real fault plane compare to equally distant stations in the direction of the auxiliary plane (Fig. 2b). Ray tracing and analysis of incident angles and take-off angles may also be used to distinguish the real fault plane from the auxiliary plane, however only the ground motion and the plunge and trend of the direction of the receiving station are used in the current work.

In practice, we have access to data from a sparse and decidedly non-uniform set of seismic stations distributed

around the Earth's curved surface, but these can yield enough control to divide the hypothetical focal sphere into quadrants of compression and dilatation if the earthquake magnitude is sufficient to cause ground motion at widely distributed stations. See Zahradnik et al. (2001), Preston et al., (2004), and Imanishi et al. (2006) for a discussion of weaker, $M < 3$, solutions). Because there are no seismic stations in the sky, we plot the lower half of the three-dimensional beach ball on a lower hemisphere stereographic projection centered on the epicenter. Beach Ball shading may be color-coded to denote focal depth using standard USGS colors (Fig. 3; see also, <http://neic.usgs.gov>).

The best fit to combined moment magnitude and orientation data for a given earthquake is called the moment tensor solution. The size of the reference sphere, and thus the radius of its stereographic projection, is arbitrary and can be used to represent the moment magnitude of the earthquake.

Data Format

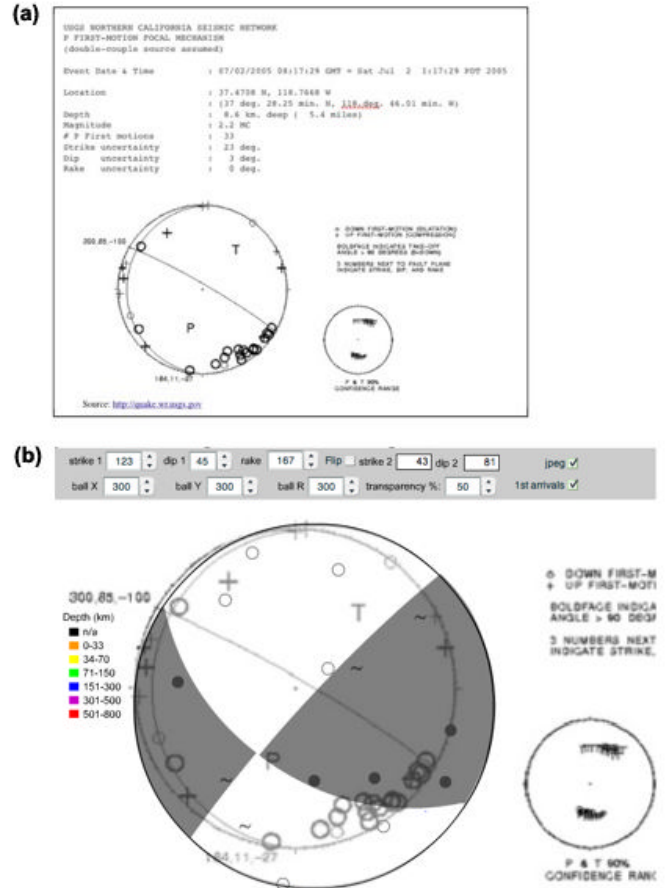
We decided to adopt an XML data schema (see Castro 2001) because of the near-universality of extensible markup language and its easy extensibility to cover the needs of sub disciplines such as geophysics (De Paor 1999, De Paor et al. 2004, 2005, Babaie & Babaei, 2002, 2003a,b,c). XML data files can be created and edited with a text editor such as Microsoft Word™. The file must be saved in the same directory as the flash swf file, with the name "data.xml". XML data files are organized by tags. A tag in XML is a string of text surrounded by angle brackets. Tags often come in pairs, e.g. "<myTag>" and "</myTag>", in which case they affect the text that they enclose. Alternatively, such opening and closing tags may be combined into one tag in which the slash comes at the end. Tags may have one or more attributes, as illustrated by the "image", "circle", and "point" tags below. Note that white space is ignored and that the order of attributes is irrelevant (compare the last "point" tag to the preceding ones.)

Example 1. An example XML document

```
<?xml version="1.0"?>
<firstMotions>
  <image file="FocMechSolnFig2.jpg" x="-5
  <stereonet Cx="300" Cy="300" Cr="300"/>
  <pole plunge="35" trend="140" symbol =
  <pole plunge="15" trend="050" symbol =
  <pole plunge="55" trend="060" symbol =
  <pole plunge="65" trend="020" symbol =
  <pole plunge="05" trend="338" symbol =
  <pole plunge="15" trend="150" symbol =
  <pole plunge="15" trend="100" symbol =
  <pole plunge="15" trend="210" symbol =
  <pole plunge="45" trend="180" symbol =
  <pole plunge="25" trend="230" symbol =
  <pole plunge="10" trend="120" symbol =
  <pole plunge="15" trend="010" symbol =
  <pole plunge="15" trend="280" symbol =
  <pole plunge="15" trend="320" symbol =
  <pole plunge="10" trend="120" symbol =
  <pole trend="190" symbol = "up" plunge=
</firstMotions>
```

In Hypertext Markup Language (HTML), tags control the format and style of a web page. For example, the sentence "this is an example" will appear on the web page as "this is an *example*". In contrast, xml tags denote content. Example 1 illustrates the tags used for our focal mechanism generator. The first tag must be the xml identifier tag, "<?xml version='1.0'?>" or equivalent. This is followed by the "<firstMotions> </firstMotions>" tag pair. Nested within the latter are three types of tag.

Figure 3. First Arrival



a) Sample web page from <http://quake.usgs.gov> showing first arrival data.

b) Image from (a) is used as a background in First-Mo.swf. Toggling the jpeg checkbox shows and hides the image. The 1st arrivals check box permits XML data to be superimposed. In practice, the jpeg stereonet would be repositioned and resized to coincide with the beach ball.

The "<image/>" tag allows a jpeg file to be loaded as a background image. Attributes specify the name of the file (which must be stored in the same directory), the coordinates of its top left corner, and a scale factor used to stretch the image equally in the horizontal and vertical directions. A background image could be an image of raw data plotted on a stereographic projection. For example, the focal mechanism solution in Fig. 3 has been constructed on top of a background image of raw first arrival data from a USGS web site. For this demonstration, the location and scale attributes have not yet been adjusted to achieve congruence of the beach ball and background stereonet. Alternatively, the background image could be a map including the event's

epicenter, as in the USGS sample in Fig. 4. The user can vary the transparency of the beach ball in order to view or hide the underlying data or map.

The second type of tag that can be nested within the firstMotion tags is the "<stereonet/>" tag. Its attributes determine the x- and y- coordinates of the center and the radius of the stereographic projection used to plot the subsequent pole data.

The third tag type is "<pole/>". Its attributes denote the plunge and trend of a receiving station and the direction of ground motion caused by the first arrival, as determined by the seismogram. Upward ground motion is rendered as a solid dot, down as an open circle, and no signal is indicated by a tilde. Pole data is plotted in equal-angle stereographic projection using the pseudo-code in Example 2.

Example 2. Example equations

$$d = Cr * \tan(\pi / 4 - \text{plunge} / 2);$$

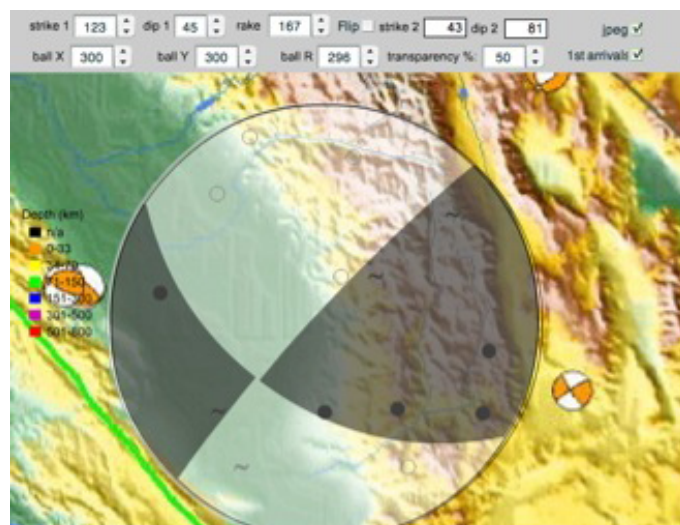
$$x = Cx + d * \cos(\text{trend} - \pi / 2);$$

$$y = Cy + d * \sin(\text{trend} - \pi / 2);$$

Fitting the Focal Mechanism to the data

Fitting of a focal mechanism to the first arrival data is performed in the shockwave flash (.swf) file called "First-Mo.swf." This is a flash movie with three frames. The first frame initializes variables and defines actionscript functions that handle the controls at the top of the window. The second frame loads the XML data, parses the tags, and projects the data. The third frame directs the movie to return to the second frame. In this way, the flash movie monitors the external data file and responds to changes whenever they are saved.

Figure 4. Example



The background image may be a geological map showing the epicenter location, for example.

With the xml data in place, the user can locate and resize the focal mechanism beach ball, varying the strike and dip of one nodal plane and the rake of the intersection with the second nodal plane. The resultant strike and dip of the second nodal plane are output (they cannot be independently altered because of the constraint of orthogonality). Pseudo-code to maintain nodal plane orthogonality is illustrated in Example 3. Black and white quadrants can be interchanged using the "flip" button and the default black color can be changed using the standard USGS color table for shallow, intermediate, and deep earthquakes.

Example 3. Pseudo-code to maintain nodal plane orthogonality

```
x = SIN(rake) * COS(dip1) * COS(strike1) - C
y = - SIN(rake) * COS(dip1) * SIN(strike1)
trend = ATAN (x / y);
plunge = ACOS(SQRT(x ^2 + y ^2));
strike2 = trend - 3 * pi / 2 modulo 2 * pi;
dip2 = pi / 2 - plunge;
```

Exporting Data

For security reasons, FirstMo.swf does not write data to the user's hard drive. To export data, users, may capture a screen shot, or use the print menu to generate a .pdf file. Options exist to show or hide the background image and

the XML data. The latter can also be hidden by decreasing the beach ball transparency. However, it is simplest to just record the best fit strike, dip, and rake data as this is all that is required for importing into rendering applications. Note that the size of the beach ball in FirstMo.swf is chosen to match the first arrival stereonet. However, to show a full moment tensor solution on a map, the focal mechanism will be resized to correspond to the event's moment magnitude.

Conclusions

The flash application presented here is intended both as a practical tool and a pedagogical aid (cf Welland 2005, Simak 2006). Focal mechanism diagrams may be rapidly generated and nodal plane data exported to other programs

and web sites for statistical study or map rendering. Students may benefit from experimenting with alternative fits of focal mechanism solutions to raw data.. This will generate discussion about what constitutes a "best fit" and what variables (strike, rake, etc.) are most sensitive to error for a particular data set (e.g. Snoke 2003).

Click [here](#) to try FirstMo.swf online. Or click [here](#) to download a zip archive containing FirstMo.swf, a sample jpeg, and a sample data.xml file. The online version has been fully tested using the Firefox web browser on WinXP and MacOSX, with the latest flash v. 8.0 plugin (v.7 or earlier will not work properly). Other web browsers and operating systems may have issues.

References

- Babaie H. A., and Babaei, A., 2002. SGeolML, an XML markup language for communication and processing of structural geological information. GSA Abstracts with Program, 34 (6).
- Babaie, H. A., and Babaei, A., 2003a. Development of the Plate Tectonics and Seismology Markup Language with XML, EGS-AGU-EUG Meeting, Nice France April 11, 2003.
- Babaie, H. A., and Babaei, A. 2003b. Applying UML and XML in designing geological markup languages. GSA Abstracts with Program, Seattle Washington, Nov. 5, 2003.
- Babaie, H. A., and Babaei, A. 2003c. The XML XSD Schema and interchange of geological data. GSA Abstracts with Program, Seattle Washington, Nov. 5, 2003.
- Castro, E., 2001. XML For the World Wide Web. Peachpit Press.
- Cronin, V., 2004. A Draft Primer on Focal Mechanism Solutions for Geologists. http://serc.carleton.edu/files/NAGTWorkshops/structure04/Focal_mechanism_primer.pdf (Vince_Cronin@baylor.edu)
- De Paor, D.G., 1999. Tectonic Markup Language – An Idea Whose Time has Come. Geological Society of American Annual Meeting, Montreal, Canada. Prog. & Abstr. 31, 115.
- De Paor, D.G., Melanson H., and Wilson, E. 2004. Analysis of structural orientation data in space and time. gsa.confex.com/gsa/2004AM/finalprogram/abstract_75232.htm
- De Paor, D. G., Morley, L., Melanson, H., and Wilson, E., 2005. Presenting Geological and Geophysical Orientation Data on Interactive Maps. Geol Soc. Amer. Paper No. 11-5.
- Imanishi, K., Cho, I., Kuwahara, Y., Hirata, N., and Panayotopoulos, Y., 2006. Focal mechanism solutions of microearthquakes around the southern part of the Itoigawa-Shizuoka Tectonic Line http://www-jm.eps.s.u-tokyo.ac.jp/2006cd-rom/pdf/S110/S110-P002_e.pdf
- Lillie, R.J., 1999. Whole Earth Geophysics – An Introductory Textbook for Geologists and Geophysicists. Prentice Hall, N.Y., 361 pp.
- Lisa, M., Khan, S.A., and Khwaja, A.A., 2004. Focal mechanism study of north Potwar de-formed zone, Pakistan Acta Seismologica Sinica, v. 17, No.3 (255–261) Article ID: 1000-9116(2004)03-0255-07. http://www.cea-igp.ac.cn/English.files/ass/ass2004/ASS_2004_3_Mona.pdf
- McNutt S. R., and Sánchez, J.J., 2000. Composite Focal Mechanisms at Four Alaskan Volcanoes. 95th annual meeting of the Seismological Society of America, 9-12 April 2000, San Diego, CA, USA.
- Preston, L., Vonseggen, D., and Smith, K., 2004. <http://www.seismo.unr.edu/greatbreak/abstracts/preston.txt>
- Sherburne, R.W., and Cramer, C., 1984. Focal mechanism studies: an explanation. California Geology, Vol. 37, No. 3.
- Simak, 2006. http://www.webpages.uidaho.edu/~simkat/course_materials/geol344/2006_4.pdf
- Snoke, J. A., 2003. FOCMEC: FOcal MECHANism determinations, International Handbook of Earthquake and Engineering Seismology (W. H. K. Lee, H. Kanamori, P. C. Jennings, and C. Kisslinger, Eds.), Academic Press, San Diego, Chapter 85.12. <http://www.geol.vt.edu/outreach/vtso/focmec/>
- USGS, 1996. <http://quake.usgs.gov/recenteqs/beachball.html>
- Weiland, C. 2005. <http://pangea.stanford.edu/GES/courses/homeworks/focalmech.html>
- Zahradnik, J., Jansky, J., Papatsimpa, K., 2001. Focal Mechanisms of Weak Earthquakes from Amplitude Spectra and Polarities, Pure and Applied Geophysics, 158, 647-665 also: <http://seis30.karlov.mff.cuni.cz/papers/aspo/aspo.html>